



ELSEVIER

Contents lists available at ScienceDirect

Materials Letters

journal homepage: www.elsevier.com/locate/matlet

Fabrication of sulfur-impregnated porous carbon nanostructured electrodes via dual-mode activation for lithium–sulfur batteries

Seung-Deok Seo, Changhoon Choi, Dong-Wan Kim*

School of Civil, Environmental and Architectural Engineering, Korea University, Seoul 136-713, South Korea

ARTICLE INFO

Article history:

Received 27 November 2015

Received in revised form

8 February 2016

Accepted 25 February 2016

Available online 27 February 2016

Keywords:

Lithium-sulfur battery

triporous carbon

Surface area

Activation process

ABSTRACT

We report the facile synthesis of a porous-carbon (PC) nanostructure via a dual-mode activation process. Its PC nanostructure, which was activated via the release of HF and NaOH during a pyrolysis of Poly(vinylidene fluoride-co-hexafluoropropylene), provided a large surface area above $2000 \text{ m}^2 \text{ g}^{-1}$. The fabricated PC was composited with sulfur via melt diffusion (PC/S), and the resulting compound was evaluated with galvanostatic cycling for use in applications of lithium–sulfur batteries. The PC/S electrode demonstrated over 730 mA h g^{-1} of reversible capacity after 100 cycles.

© 2016 Elsevier B.V. All rights reserved.

1. Introduction

Advanced lithium–sulfur batteries (LSBs) are a promising technology for next-generation energy-storage devices for both small- and large-scale applications. Theoretically, they have the three-to-five-fold greater specific energy (2500 Wh kg^{-1}) than conventional lithium-ion batteries (LIBs) [1]. Furthermore, elemental sulfur is exceptionally cost competitive as compared to conventional cathode materials based on transition-metal oxides [2].

However, despite their remarkable superiority over LIBs, LSBs have not yet been commercialized because of several intrinsic limitations to their widespread application. Preferentially, elemental sulfur has low electric conductivity slightly better than that of an insulator ($5 \times 10^{-30} \text{ S cm}^{-1}$ at $25 \text{ }^\circ\text{C}$), which hinders the good electrochemical contact of the active materials and provokes low sulfur utilization in the cathode [3]. Furthermore, the reaction intermediates, lithium polysulfide molecules, are highly soluble in organic electrolytes and easily reduce on the lithium-anode surfaces. This shuttle mechanism and the reduced lithium polysulfides generate lithium-anode degradation and unwanted electrochemical reactions that lower the cyclic efficiency of a cell [4].

Porous-carbon materials have been considered a powerful solution of these practical drawbacks and a further enhancement of sulfur cathodes. The microtextures of porous carbon act both as a container of active sulfur and as a conducting pipeline because of the interconnected internal pore structures [5]. In this study, we

fabricated porous-carbon (PC) nanostructures via a simple one-step pyrolysis process from a commercial Poly(vinylidene fluoride-co-hexafluoropropylene) (PVdF-HFP), which goes by the commercial name Kynar 2801. Furthermore, the porous-carbon–sulfur (PC/S) composite samples were synthesized via melt diffusion of commercial sulfur powder. The electrochemical properties of the PC/S samples were also investigated as promising electrodes for LSBs.

2. Experimental sections

The PC samples were synthesized via a simultaneous pyrolysis and activation process of the Kynar 2801 polymer (PVdF-HFP, $M_w = 380,000$, ca. 11–12% HFP, Arkema) with sodium hydroxide (NaOH, Sanchun). First, 1 g Kynar 2801 and 3.5 g NaOH powder were sufficiently blended and transferred to a horizontal tube furnace, and the pyrolysis process occurred at $600 \text{ }^\circ\text{C}$ for 1 h under 100 sccm of a N_2 gas flow. After the carbonization, the powders were acid-treated, washed, and dried at $120 \text{ }^\circ\text{C}$. The PC/S composite samples were synthesized via melt diffusion of commercial sulfur powder. Sublimed sulfur powder (S, Alfa Aesar) and a PC sample were mixed in a ratio of four to one, and the melt-diffusion process was performed at $155 \text{ }^\circ\text{C}$ for 12 h under 100 sccm of Ar gas flow [5].

We investigated the morphologies and pore structures of the PC and PC/S samples using field-emission scanning electron microscopy (FESEM, S-4300, Hitachi) and field-emission transmission electron microscopy (FETEM, Tecnai G² F30 ST, FEI). The surface areas of both composites were measured via the

* Corresponding author.

E-mail address: dwkim1@korea.ac.kr (D.-W. Kim).

Brunauer–Emmett–Teller (BET) method using the N₂-adsorption analyzer (ASAP-2020, Micrometrics). The pore size distributions and pore volumes were calculated via the Barrett–Joyner–Halenda (BJH) and Horvath–Kawazoe (HK) methods, respectively. The surface-bonding chemistry was analyzed via Fourier transform infrared spectroscopy (FTIR, LabRam ARAMIS IR2, HORIBA Jobin Yvon). The weight ratio of sulfur in the composite was analyzed by utilizing a thermogravimetric analysis (TGA, DTG-60A, Shimadzu).

The electrochemical performances of the PC/S powders were investigated by assembling Swagelok-type half-cells, which consisted of working electrodes, counter electrodes, and separator film (Celgard 2400, Celgard) with a liquid electrolyte of 1 m lithium-bis-(trifluoromethanesulfonyl)-imide (LiTFSI, Sigma-Aldrich) and 0.2 m lithium nitrate dissolved in a 1:1 (v:v) mixture of dimethoxyethane (DME, Sigma-Aldrich) and dioxolane (DOL, Sigma-Aldrich). The working electrodes were prepared using the active material (pristine S, PC/S), a conducting additive (Super P, MMM carbon), and a binder (Kynar 2801) with a weight ratio of 8:1:1. The active amount of sulfur on electrode is 1.5 ± 0.2 mg. The assembled cells were galvanostatically cycled between 1.0 and 3.0 V of a voltage window under 0.1C of current rate ($1C = 1.6 \text{ A g}^{-1}$) using a battery cycler (MACCOR 4000, Maccor).

3. Results and discussion

We conducted the facile syntheses of macro-, meso-, and micro-structured PC via a one-step dual-activation process, as shown in Fig. 1. The PVdF-HFP contains numerous carbon, hydrogen, and fluorine atoms that tightly make up the polymeric chain. We made good use of both decomposition and carbonization of the polymer chain under certain conditions with simultaneous activation by using NaOH. As delineated in Fig. 1, during the pyrolysis process of PVdF-HFP described above, molecules of hydrofluoric acid (HF) escaped from the polymer matrix, and this phenomenon created voids in the said matrix. In these results, a polymer-based matrix became a group of pyrolytic carbon structures with numerous voids (pores), which had nonuniform size distributions [6]. Furthermore, premixed NaOH also plays an important role during the pyrolytic-carbonization process. The NaOH in the mixture induced an activation of the carbon frameworks, like as the typical alkaline activator KOH ($6\text{KOH} + 2\text{C} \rightarrow 2\text{K} + 2\text{K}_2\text{CO}_3 + 3\text{H}_2$) [7]. Instead of KOH with high reactivity, the NaOH was used to prevent an excess activation forming relatively large pore structure upon carbonization. After the carbonization and activation process, we infiltrated sulfur into the PC using the melt-diffusion method at 155 °C.

In Fig. 2(a), we can easily observe the well-developed macro- and mesoporous structures that surround the relatively large (> 500 nm) pores from the FESEM images. According to the aforementioned mechanism of alkali activation, after NaOH

reacted with carbon atoms, sodium and sodium carbonate remained as reaction residues. When the submicron-sized residues were removed by several rounds of washing, macroporosity emerged. Carbon nanostructure had an irregular lump-like shape, and there are many wavy, macro- and meso-sized pores on the surface, as shown in Fig. 2(b). The upper- and lower-inset images show enlarged views of the selected region in Fig. 2(b), which depicts the detailed morphology of the wavy, hierarchical, mesoporous structure and disordered, microporous structures of the entire carbon structure, which resulted from NaOH activation. In the FETEM image, the micropores do not distinctly differ from common amorphous carbon, but there are some similar studies concerning microporous carbon that report almost the same morphology as we do here [8]. Because of these results, we can accept that the PVdF-HFP-derived carbon possessed triporous nanostructures. The FESEM image in Fig. 2(c) shows a typical high-magnification image of the PC/S composite in which the pores are closed by the melt-diffused, amorphous sulfur. The FETEM image of PC/S in Fig. 2(d) displays a plane view of the structure of the composite, consisting of amorphous sulfur on the PC surface. The porous-carbon nanostructure has a mottled surface with no evident original pore structures. In the energy-dispersive X-ray diffraction (EDS) results shown in the inset, we verified that the elemental sulfur was well diffused into every pore structure and surface on the PC. Contrary to crystalline pristine sulfur, the diffraction patterns of the TPC/S composite show several broad and tiny peaks, meaning that the sulfur was completely diffused into the TPC matrix in an amorphous form, owing to the synthesis temperature (Fig. S1).

By comparing the mass loss between the PC and PC/S composite using TGA, the amount of sulfur in the composite corresponded to about 60%, as shown in Fig. 3(a). The FTIR spectra in Fig. 3(b) well described the phase transition of PVdF-HFP as it became a composite with sulfur. The peaks of PVdF ($750\text{--}1500 \text{ cm}^{-1}$) [9] disappeared after pyrolysis. We further investigated the pore structures of PC, which facilitated the significant mass loading of sulfur, that were derived from the PVdF-based copolymer. Fig. 3(c) displays the N₂ isotherm of the PC and PC/S composite. The N₂ physical adsorption–desorption curve of the PC shows mixed types of I and IV, which refer to the microporosity and diverse pore size distribution in a range of 1–100 nm [10]. The pore distribution of the PC, depicted in a BJH pore distribution, and the HK plot on the right side support this N₂ isotherm. The upper-right side of this figure shows the BJH desorption plot of the PC. It shows the pore distribution, which included micro-, meso-, and macropores. Additionally, the HK plot under 4 nm depicts the existence of micropores under 1 nm in size, derived from the HF removal during the pyrolysis process. For these reasons, the as-synthesized PC had a large BET surface area ($2139 \text{ m}^2 \text{ g}^{-1}$), total pore volume ($1.95 \text{ cm}^3 \text{ g}^{-1}$), and average

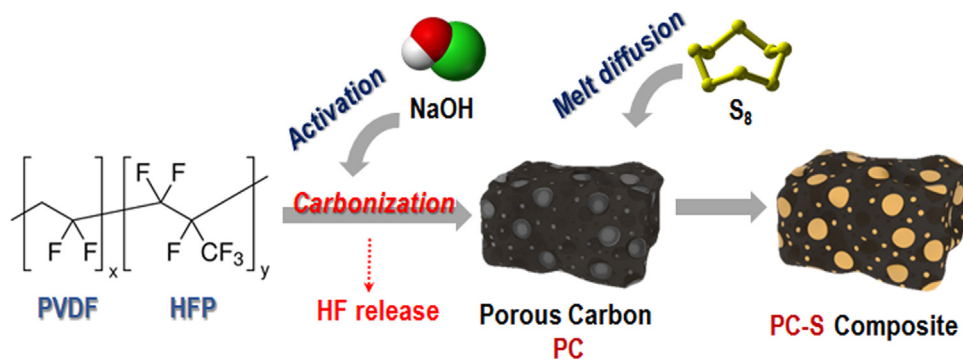


Fig. 1. Synthetic process of porous carbon (PC) from PVdF-HFP.

Download English Version:

<https://daneshyari.com/en/article/1641551>

Download Persian Version:

<https://daneshyari.com/article/1641551>

[Daneshyari.com](https://daneshyari.com)